PHYSICAL REVIEW E, VOLUME 65, 035107(R)

Crack propagation in thin glass plates caused by high velocity impact

Toshihiko Kadono[1,*] and Masahiko Arakawa[2]
[1]*Earthquake Research Institute, University of Tokyo, Tokyo 113-0032, Japan*
[2]*Institute of Low Temperature Science, Hokkaido University, Sapporo 060-0819, Japan*
(Received 9 October 2001; published 6 March 2002)

Crack propagation within thin glass plates under high shock loading is directly observed using a high speed camera. The fractal dimension of cracks and the power-law exponents of the fragment area distributions are investigated as a function of time. Two models of the fragmentation process are proposed: in one case the cracks are netlike, while in the other the cracks are treelike, and the relations between fractal dimension and power-law exponent are estimated and compared with the experimental results. It appears that at early stages of the fragmentation process the relation is described by the latter case, while at later stages it approaches that of the former case.

DOI: 10.1103/PhysRevE.65.035107 PACS number(s): 46.50.+a, 62.20.Mk, 64.60.Ak

Fragmentation of brittle solids has been investigated for many decades because of its importance in various fields of science and engineering. Experiments have been carried out for objects of different materials such as glass [1], rock [2], and ice [3], and for various shapes [4,5]. Fragment size distributions are extensively studied because they provide the primary observational evidence for the nature of the breakup process. Experiments indicate that one of the characteristic features of fragment size distributions is that the distribution in the small size range shows a power-law form. The origin of this power law has attracted much attention and some analytical approaches have been made [6–11]. Also, several models have been introduced to study fragmentation numerically [12–18].

One effective method to clarify the origin of the power law is the direct observation of the fragmentation process. In some experiments, the fragmentation process has been observed directly. Failure waves in glass bars and plates have been investigated using a high speed camera [19]. Also, the propagation of large radial cracks in H_2O ice targets has been observed and the expansion velocity of the fractured region has been measured with an apparatus consisting of an image-converter camera and a shadow photograph lighting system [20]. However, fragment size distributions were not discussed in these studies.

Here we report the results of hypervelocity impact experiments using thin transparent plate targets, in which individual cracks are directly observed without the overlap of many cracks in the line of sight. Recently, the relation between crack systems and the power-law form has been often discussed [15,21]. Hence, initially, fractal dimension as a parameter characterizing the crack systems is estimated as a function of time. Second, fragment size distributions are investigated as a function of time. Finally the relation between fractal dimension and the power-law exponent of fragment size distributions is discussed.

A schematic view of the experimental system is shown in Fig. 1. Thin Pyrex glass plate targets were vertically installed and suspended by two fine threads under an ambient pressure of 1 atom. Cylindrical aluminum projectiles with a diameter of 15 mm and a height of 10 mm, which were accelerated by an air-gun at Institute of Low Temperature Science, impacted against the upper side of the targets. Around the impact point, two brass semicircular projectile stoppers with a radius of 15 mm and a thickness of 10 mm were set to prevent the projectile from penetrating into the target. These stoppers are connected by two thin threads and hooked on the upper side of the target. The projectile initially impacts the target, and its motion is quickly terminated by the stoppers.

Crack propagation was observed using an image converter camera, ULTRA NAC. Cracks could be observed by means of a shadow photograph lighting system. A xenon flash lamp (flash duration longer than 1 ms) was used for the light source. The camera view is almost normal to the target plane but slightly inclined to enhance the contrast of crack images.

Figure 2 shows a result using a square glass plate target with sides of 100×100 mm and a thickness of 2 mm. The image converter camera recorded 9 successive images with a framing speed of 1×10^5 frames per second (10 μs per frame) and an exposure time of 800 ns. Numbers in the figure are the order of the images. The projectile impacted against the center of the upper side at an impact velocity of 67.6 m/s. The black square on the upper side of the target is the projectile.

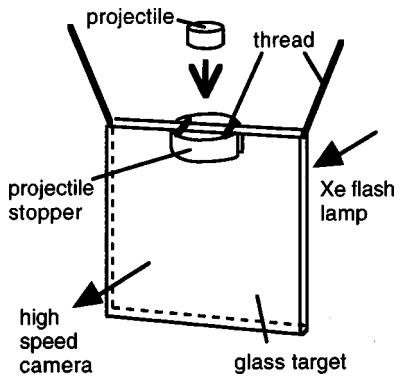

FIG. 1. A schematic view of the experimental system.

*Author to whom correspondence should be addressed. FAX: 81-3-5802-3391. Email address: kadono@eri.u-tokyo.ac.jp

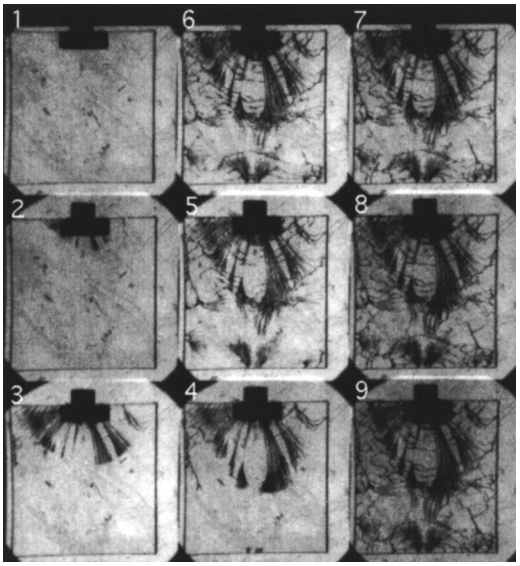

FIG. 2. Consecutive images. Framing speed is 10 μs per frame. Numbers in the figure are the order of the images. A cylindrical projectile is shot from the top at an impact velocity of 67.6 m/s.

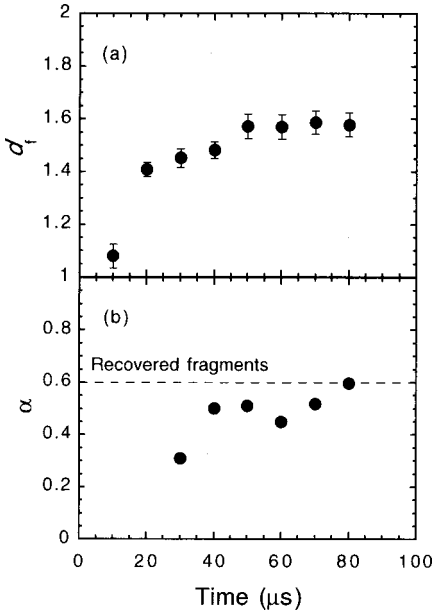

FIG. 3. (a) Fractal dimension of the crack system as a function of time. (b) Slope α of fragment area distributions as a function of time.

The propagation of individual cracks could be observed. At first, some radial cracks proceeded downward from the impact point with branching. Then a few cracks generated at the antipodal side (lower side) of the target and proceed upward with branching. After that, these branching cracks coalesced with each other, and lateral cracks perpendicular to the radial cracks appeared.

The fractal dimension of cracks d_f was estimated in each image using the box counting method [22]. The number of boxes which are necessary to cover all crack branches was counted. The minimum box size corresponded to about a half of the target thickness and the range of the box size was over one order of magnitude. In Fig. 3(a) the results are plotted against the time t. The time 0 corresponds to the frame 1. As t increases, d_f increases quickly and becomes about 1.5.

After the shot, the fragments were recovered. In Fig. 4 we plot the cumulative number of the recovered fragments with mass larger than m as indicated by a bold line. The fragment mass is normalized by the original target mass. The distribution shows a power-law form in the small-size range. The slope of the power-law region is 0.60 ± 0.01.

Then the fragment area distributions in each image are obtained by defining a ''fragment'' as a closed part surrounded by cracks. Figure 4 also shows the cumulative number $N(>s)$ of fragments with areas larger than s, where area s is normalized by the original target area. It appears that the number of fragments increases with time and that the distributions after frame 7 are close to that of the recovered fragments. In small fragments, the distribution of recovered fragments is slightly higher than those obtained from the images. This is probably because the distribution of recovered fragments includes some ''3D fragments'' which are produced mainly around the impact point and whose thickness is usually less than that of the original target plate: these fragments cannot be counted by image analysis. Also, since the target is slightly inclined to enhance the contrast, the cracks have some ''width'' in the image. Therefore the estimated area of a fragment is smaller than the actual value. Smaller fragments are more strongly affected. Consequently, the cumulative number distributions obtained by the image analysis become slightly lower in the small-size limit.

We fit the part indicating a power-law form in each distribution to a straight line and obtained its slope α. We did not fit the distribution in the frame 3 because the number of fragments is so small that the part indicating a power-law form is not clear. Figure 3(b) shows α against t. The slope α also increases with time and approaches that for the recovered fragments indicated by a broken line.

Figure 5 shows d_f against α. Other results obtained at a similar impact velocity (72.3 m/s) are also shown. In this case, the framing speed is relatively slower (15 μs per frame), and hence the time evolution of d_f and α at early stages could not be observed. Furthermore, the fractal dimensions for plaster targets [5] are plotted, which are esti-

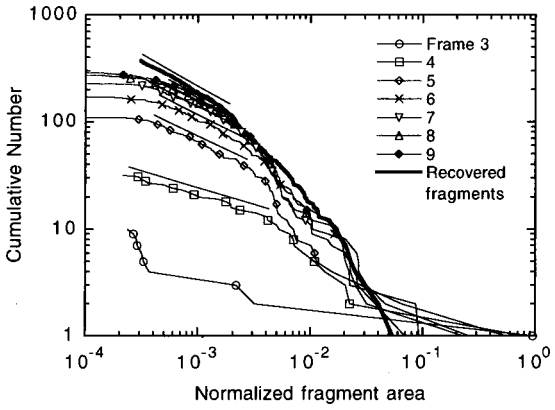

FIG. 4. Cumulative number of fragments $N(>s)$ as a function of time. That of recovered fragments is also shown.

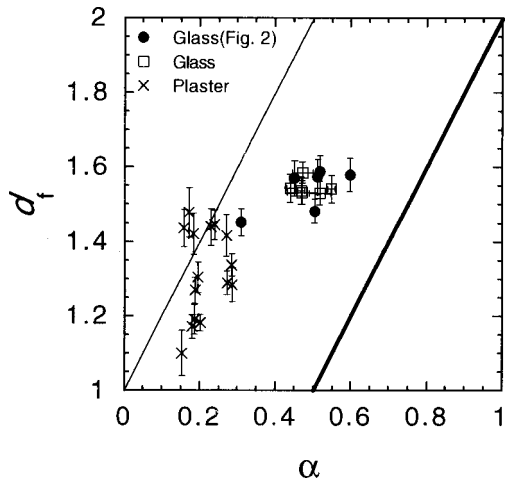

FIG. 5. Power-law exponents α versus fractal dimensions d_f. The previous results [5] are also shown. The bold line is obtained from model 1 and the thin line is from model 2.

mated from a sketch of crack patterns obtained by reconstructing the recovered fragments, as shown in Fig. 1(b) of Ref. [5]. It appears that d_f increases with α.

Here the relation between d_f and α is discussed briefly. We propose two simple models of the fragmentation process. First we consider a process which is analogous to the Sierpinski-constructions [8] (model 1). In two-dimensional space we take a square with a side of unit length [Fig. 6(a)]. As a first step, we divide the square into b^2 subsquares of side $1/b$ [in Fig. 6(a), $b=2$]. At the second step we take b^2p subsquares, where p is the fraction of the subsquares which will be further fragmented, and divide each into b^2 equal sub-subsquares of side $(1/b)^2$ [in Fig. 6(a), $p=3/4$]. By repeating the procedure, we obtain a collection of an infinite number of fragments of various sizes. The number of fragments with a length of $r_n=(1/b)^n$ is $(pb^2)^{n-1}(1-p)b^2$. Hence the cumulative number of fragments larger than r_n, $N(>r_n)$, becomes

$$\begin{aligned} N(>r_n) &= (1-p)\times b^2+(pb^2)\times(1-p)\times b^2+\cdots \\ &\quad +(pb^2)^{n-1}\times(1-p)\times b^2 \\ &\sim (pb^2)^n \\ &= r_n^{-A}, \end{aligned}$$

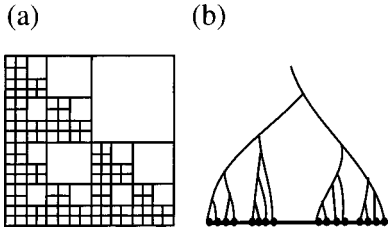

FIG. 6. (a) Model 1. A fragmentation process analogous to the Sierpinski constructions introduced in Ref. [8]. (b) Model 2. Fragments caused by the intersections of a crack with a fractal dimension d_f with a straight line.

where $A=\ln(b^2p)/\ln b$. This can be rewritten as the cumulative number of fragments larger than $s=r^2$, $N(>s)\sim s^{-\alpha}\sim s^{-A/2}$.

In the process of the box counting method the total number $n(r_n)$ of boxes of size r_n needed to cover a fractal structure of dimension d_f is given by $n(r_n)\sim r_n^{-df}$. In this model, for the boxes of size $r_{n+1}=r_n/b$, $n(r_{n+1})$ is larger by a factor pb^2 than $n(r_n)$. Hence the fractal dimension d_f can be written as $d_f=\ln(b^2p)/\ln b$. Thus we obtain $A=d_f$ and hence $\alpha=d_f/2$. This is shown as a bold line in Fig. 5. There are no experimental results which correspond to this line.

Next we consider another case: a branching crack intersects a line as shown in Fig. 6(b) (model 2). This line may be a free surface (in the case of platelike objects it is a side) or a part of already existing cracks. It is expected that the length between two adjacent intersections represents the size of a fragment. Hence, we obtain the cumulative number of fragments larger than r as the cumulative number of segments longer than r.

First we take a line with a unit length. A crack divides the line into b segments of length $1/b$ [in Fig. 6(b), $b=3$]. Letting p be the fraction of the segments which are further fragmented [in Fig. 6(b), $p=2/3$], bp segments are divided into b equal subsegments of length $(1/b)^2$ by the crack. Finally, we obtain a collection of an infinite number of segments of various lengths. The number of segments with a length of $r_n=(1/b)^n$ is $(pb)^{n-1}(1-p)b$. Hence the cumulative number of segments longer than r_n, $N(>r_n)$, becomes

$$\begin{aligned} N(>r_n) &= (1-p)\times b+(pb)\times(1-p)\times b+\cdots+(pb)^{n-1} \\ &\quad \times(1-p)\times b \\ &\sim (pb)^n \\ &= r_n^{-B}, \end{aligned}$$

where $B=\ln(bp)/\ln b$.

In a way similar to model 1, the total number $n(r_{n+1})$ of boxes of size $r_{n+1}=r_n/b$ needed to cover the intersections is estimated to be larger by a factor pb than $n(r_n)$. Hence the fractal dimension D of the distribution of the intersections can be written as $D=\ln(bp)/\ln b$. Thus we obtain $B=D$. Since the fractal dimension of the crack d_f is related to D by $d_f=1+D$, we obtain $B=d_f-1$ and hence $\alpha=(d_f-1)/2$. This is also shown in Fig. 5.

For small α the experimental data in plaster plates and in glass plates at early stages exist near the line $\alpha=(d_f-1)/2$, though the data for plaster slightly scatter. The data for glass at late stages deviate from the line. They exist around the middle of two lines.

Qualitatively speaking, at early stages where only a few treelike cracks exist, the fragmentation process is described by model 2, while at later stages where cracks coalesce with each other and are not treelike but netlike, the fragmentation process approaches that represented by model 1. In the case of plaster targets, since the stress waves attenuate quickly it seems that the fragmentation stops at an early stage.

In summary, impact fragmentation experiments are carried out using thin glass plates. Crack propagation is directly observed with a high speed camera. The fractal dimensions of cracks and the power-law exponent of the fragment area distributions are investigated as a function of time. Two models of fragmentation process are proposed: in one case the cracks are netlike, while in the other the cracks are treelike, and the relations between fractal dimension and power-law exponents are estimated and compared with the experimental results. It seems that at early stages of the fragmentation process the relation is described by the latter case while at later stages it approaches that in the former case.

The authors would like to thank D. Tomizuka, S. Nakatsubo, and S. Nakazawa for assisting in the experiments and N. K. Mitani, S. Sugita, and M. Higa for their helpful comments.

[1] J. J. Gilvarry and B. H. Bergstrom, J. Appl. Phys. **32**, 400 (1961); D. E. Gault and J. A. Wedekind, J. Geophys. Res. **74**, 6780 (1969).

[2] A. Fujiwara, G. Kamimoto, and A. Tsukamoto, Icarus **31**, 277 (1977); T. Matsui, T. Waza, K. Kani, and S. Suzuki, J. Geophys. Res. **87**, 10 968 (1982); Y. Takagi, H. Mizutani, and S. Kawakami, Icarus **59**, 462 (1984).

[3] M. A. Lange and T. Ahrens, in Proceedings of the Twelfth Lunar and Planetary Science Conference, Proceedings of Lunar and Planetary Science [Geoch. Cosmochim. Acta **12B**, Suppl. 16, 1667 (1981)]; M. Kato, Y. Iijima, M. Arakawa, Y. Okimura, A. Fujimura, N. Maeno, and H. Mizutani, Icarus **113**, 423 (1995).

[4] T. Ishii and M. Matsushita, J. Phys. Soc. Jpn. **61**, 3474 (1992); L. Oddershede, P. Dimon, and J. Bohr, Phys. Rev. Lett. **71**, 3107 (1993); Z. Neda, A. Mocsy, and B. Bako, Mater. Sci. Eng., A **169**, L1 (1993); A. Meibom and I. Balslev, Phys. Rev. Lett. **76**, 2492 (1996).

[5] T. Kadono, Phys. Rev. Lett. **78**, 1444 (1997).

[6] J. J. Gilvarry, J. Appl. Phys. **32**, 391 (1961).

[7] D. E. Grady and M. E. Kipp, Int. J. Rock Mech. Min. Sci. Geomech. Abstr. **17**, 147 (1980).

[8] M. Matsushita, J. Phys. Soc. Jpn. **54**, 857 (1985).

[9] D. L. Turcotte, J. Geophys. Res. **91**, 1921 (1986); A. C. Palmer and T. J. O. Sanderson, Proc. R. Soc. London, Ser. A **433**, 469 (1991); S. J. Steacy and C. G. Sammis, Nature (London) **353**, 250 (1991); M. Marsili and Y.-C. Zhang, Phys. Rev. Lett. **77**, 3577 (1996).

[10] R. Englman, N. Rivier, and Z. Jaeger, Philos. Mag. B **56**, 751 (1987); R. Englman, J. Phys.: Condens. Matter **3**, 1019 (1991).

[11] A. Z. Mekjian, Phys. Rev. Lett. **64**, 2125 (1990).

[12] U. Naftaly, M. Schwartz, A. Aharony, and D. Stauffer, J. Phys. A **24**, L1175 (1991).

[13] G. Hernandez and H. J. Herrmann, Physica A **215**, 420 (1995).

[14] Y. Hayakawa, Phys. Rev. B **53**, 14 828 (1996).

[15] J. Åström, M. Kellomäki, and J. Timonen, Phys. Rev. E **55**, 4757 (1997); J. Åström and J. Timonen, Phys. Rev. Lett. **78**, 3677 (1997).

[16] H. Inaoka and H. Takayasu, Physica A **229**, 5 (1996); H. Inaoka, E. Toyosawa, and H. Takayasu, Phys. Rev. Lett. **78**, 3455 (1997).

[17] E. S. C. Ching, Y. Y. Yiu, and K. F. Lo, Physica A **265**, 119 (1999).

[18] F. Kun and H. J. Herrmann, Phys. Rev. E **59**, 2623 (1999); J. A. Åström, B. L. Holian, and J. Timonen, Phys. Rev. Lett. **84**, 3061 (2000); A. Diehl, H. A. Carmona, L. E. Araripe, J. S. Andrade, Jr., and G. A. Farias, Phys. Rev. E **62**, 4742 (2000).

[19] N. S. Brar, S. J. Bless, and Z. Rosenberg, Appl. Phys. Lett. **59**, 3396 (1991); S. J. Bless, N. S. Brar, G. Kanel, and Z. Rosenberg, J. Am. Ceram. Soc. **75**, 1002 (1992).

[20] M. Arakawa, N. Maeno, and M. Higa, J. Geophys. Res. **100**, 7539 (1995); M. Arakawa, K. Shirai, and M. Kato, Geophys. Res. Lett. **27**, 305 (2000).

[21] E. Sharon and J. Fineberg, Phys. Rev. B **54**, 7128 (1996); E. Sharon and J. Fineberg, Philos. Mag. B **78**, 243 (1998).

[22] T. Vicsek, *Fractal Growth Phenomena* (World Scientific, Singapore, 1992).